Journal of the Meteorological Society of Japan, Vol. 90, No. 4, pp. 535−552, 2012
DOI: 10.2151/jmsj.2012-407

Differences in Teleconnection over the North Pacific and Rainfall Shift over the USA Associated with Two Types of El Niño during Boreal Autumn

Wenjun ZHANG

Key Laboratory of Meteorological Disaster of Ministry of Education and College of Atmospheric Sciences, Nanjing University of Information Science & Technology, Nanjing, China
School of Ocean and Earth Science and Technology, University of Hawaii, Honolulu, Hawaii, USA

Fei-Fei JIN, Hong-Li REN

School of Ocean and Earth Science and Technology, University of Hawaii, Honolulu, Hawaii, USA

Jianping LI

LASG, Institute of Atmospheric Physics, Chinese Academy of Sciences, Beijing, China

and

Jing-Xia ZHAO

School of Ocean and Earth Science and Technology, University of Hawaii, Honolulu, Hawaii, USA

(Manuscript received 26 January 2012, in final form 12 May 2012)

Abstract

This work investigates the teleconnection patterns over the North Pacific/North America sector and regional rainfall variability over the southwestern USA during boreal autumn, associated with two types of El Niño. These two types, called cold tongue (CT) and warm pool (WP) El Niños, have an opposing impact on atmospheric circulation over the eastern North Pacific. When CT El Niño occurs, a strong cyclonic anomaly tends to appear over the North Pacific, and the associated southwesterly winds bring unusually moist air and thereby enhance rainfall over the southwestern USA. However, during WP El Niño autumns, a tripolar anomaly develops over the North Pacific. The associated northerly and northeasterly winds transport unusually dry air to the southwestern USA causing a reduction in rainfall. In this region, the rainfall response to WP El Niño is similar to that of La Niña, but opposite to that of CT El Niño.

Since the early 1990s, the WP El Niño event has occurred more frequently, while the CT El Niño events has become less. The La Niña events remain roughly unchanged in terms of the zonal location. Autumn rainfall deficits over the southwestern USA have also been more frequent after the 1990s. The El Niño regime change thus appears to contribute to a decadal difference in the regional autumn rainfall.

Corresponding author: Wenjun Zhang, College of Atmospheric Sciences, Nanjing University of Information Science and Technology, Nanjing 210044, China.
E-mail: zhangwj@nuist.edu.cn

1. Introduction

The El Niño–Southern Oscillation (ENSO) is one of the most important low-frequency phenomena arising from coupled ocean–atmosphere interactions in the tropical Pacific (Bjerknes 1969; Wyrtki 1975; Cane and Zebiak 1985; Schopf and Suarez 1988; Battisti and Hirst 1989; Jin 1997a, b; Neelin et al. 1998; Wang and Picaut 2004). Many studies have reported ENSO variations with its complex and highly variable characteristics (Neelin et al. 1998; Trenberth and Stepaniak 2001; Jin et al. 2003; Bejarano and Jin 2008; Zhang et al. 2009). In the last decade, some studies have argued that there exists a new type of El Niño in the tropical Pacific, whose action center of sea surface temperature (SST) anomaly (SSTA) is located near the dateline in the central equatorial Pacific (Larkin and Harrison 2005a, b; Ashok et al. 2007; Kao and Yu 2009; Kug et al. 2009). This differs markedly from the conventional (or canonical) El Niño, for which the strongest variability of the associated atmosphere and ocean is confined to the eastern equatorial Pacific (Rasmusson and Carpenter 1982; Wallace et al. 1998).

Following a new definition of El Niño issued by the National Oceanic and Atmospheric Administration (NOAA) in 2003, a number of additional El Niño events were identified by Larkin and Harrison (2005a, b), which go beyond the conventional definition. They referred to these events as "dateline El Niño" because the SSTA center is located near the dateline. Ashok et al. (2007) argued that a new type of El Niño may exist in the tropical Pacific, based on the second empirical orthogonal function (EOF) mode. This type, which they called "El Niño modoki", is characterized by a warming SSTA in the central Pacific and a cold SSTA in the western and eastern Pacific. Kao and Yu (2009) separated this new type of El Niño from the conventional El Niño through EOF and linear regression analyses, and they named the new type of El Niño, the "central Pacific El Niño." Based on SSTA spatial patterns, Kug et al. (2009) categorized El Niño events into two groups with different dynamical processes. In their study, "warm pool El Niño" was used to describe events with maximum warming in the central Pacific, since the action center of anomalous SST and atmosphere is located mainly at the eastern edge of the warm pool. In these previous studies, it appears that a similar phenomenon has been discussed in each case; however, different nomenclatures have been used to describe the new type of El Niño. In fact, most of the events associated with the new type of El Niño have been consistently selected based on these different definitions (Ashok et al. 2007; Kao and Yu 2009; Kug et al. 2009; Ren et al. 2011). Here, we refer to the new type and conventional El Niño as the warm pool (WP) and cold tongue (CT) El Niño respectively, following Kug et al. (2009) and Ren and Jin (2011).

ENSO has received extensive public attention because of its significant global climatic impacts (van Loon and Madden 1981; Ropelewski and Halpert 1987, 1996; Trenberth and Caron 2000). One prominent teleconnection associated with ENSO that has an important influence on the North American winter climate, has been referred to as the Pacific–North America (PNA) pattern (Hoskins and Karoly 1981; Wallace and Gutzler 1981). The PNA teleconnection pattern is characterized by a wave-train from the tropical Pacific to North America. During the canonical El Niño condition, the PNA pattern exhibits above-average heights over the subtropical Pacific near Hawaii and the inter-mountain region of North America, and below-average heights south of the Aleutian Islands and over the southeastern USA. The Pacific–East Asian (PEA) teleconnection was proposed by Wang et al. (2000) to link the East Asian climate to El Niño through anomalous anticyclones over the western North Pacific (WNP). The WNP anticyclone can cause wet anomalies over southern China during winter. However, different global teleconnection patterns are found with the two types of El Niño during boreal winter which can result in differences in regional rainfall anomalies (Larkin and Harrison 2005a, b; Weng et al. 2009; Feng et al. 2010; Mo 2010). For example, during the CT El Niño winter, anomalous low pressure occurs over the North Pacific, whereas anomalous high pressure is found near 50°N during the new type of El Niño winter (Weng et al. 2009). Differing Walker Circulation and Philippine anticyclone anomalies tend to cause different rainfall anomaly patterns over Southeast Asia (Feng et al. 2010).

Differences in atmospheric behavior during other seasons are also found to be distinctly associated with the two types of El Niño (Larkin and Harrison 2005a, b; Wang and Hendon 2007; Weng et al. 2007; Cai and Cowan 2009; Kim et al. 2009; Taschetto and England 2009; Chen and Tam 2010; Feng and Li 2011; Hong et al. 2011). A pattern like the PNA is seen to appear over the eastern Pacific and North America during the WP El Niño summer, whereas, this pattern is not evident during the CT El Niño summer (Weng et al. 2007). Temperature and rainfall anomalies associated with the two types of El Niño differ markedly over most regions of the USA during boreal autumn (Larkin and Harrison 2005a, b). The two types of El Niño have a dif-

fering influence on spring rainfall over southern China through different teleconection patterns (Feng and Li 2011). There is a greater-than-average frequency of tropical cyclones along the Gulf of Mexico coast and Central USA during a WP El Niño year, compared with a lower-than-average frequency for a CT El Niño year (Kim et al. 2009). Compared with a normal year, the tropical cyclones occur more frequently over the WNP during the WP El Niño, whereas tropical cyclone frequency is reduced over the northern portion of the WNP and enhanced over the southern area during the CT El Niño (Chen and Tam 2010).

The two types of El Niño have contrasting impacts on the WNP atmospheric circulation during boreal autumn, and thus on autumn rainfall over southern China; however, these differences tend to diminish during subsequent seasons (Zhang et al. 2011). Here, we consider whether the autumn teleconnection pattern over the North Pacific during the WP El Niño differs markedly from that during the CT El Niño. This issue deserves attention because of important impacts on climate over the USA (e.g., Larkin and Harrison 2005a, b). In this study, we investigate the teleconnection patterns of these two types of warming events over the North Pacific/North America region during the boreal autumn, and for comparison, we consider the autumn teleconnection patterns during La Niña events and their associated regional rainfall responses, as investigated in previous studies (e.g., Ropelewski and Halpert 1996; Larkin and Harrison 2001). This study provides new knowledge by taking a recent mainstream approach, although a similar perspective is shown in previous studies.

WP El Niño events have occurred more frequently since the early 1990s (Ashok et al. 2007; Kug et al. 2009; Yeh et al. 2009). In the same period, autumn drought has become more common over southern China (Niu and Li 2008). For example, during the 2004 and 2009 WP El Niño autumns, southern China experienced severe droughts with disastrous effects on the supply of domestic and agricultural water. Therefore, ENSO changes may be responsible for regional climate change, such as autumn rainfall activity. In the present work, we also investigate the southwestern USA to explore decadal differences in autumn rainfall associated with ENSO changes.

The remainder of this manuscript is organized as follows. Section 2 introduces the data and Section 3 compares the teleconnection patterns of the two types of El Niño in the boreal autumn. Section 4 explores the regional autumn rainfall anomalies and their decadal change associated with ENSO events. Finally, a discussion and conclusion are presented in Section 5.

2. Data and methods

The monthly SST datasets employed in this study are the global sea ice and sea surface temperature analyses from the Hadley Center (HadISST1) (1951–2009) (Rayner et al. 2003). Re-analyses from the National Centers for Environmental Prediction (NCEP) (1951–2009) (Kalnay et al. 1996) were used to identify ENSO-related teleconnection patterns. The monthly station rainfall data for the USA (1951–2009) are from the United States Historical Climatology Network (Karl et al. 1990), and rainfall data were also obtained from the Global Precipitation Climatology Centre (GPCC) (Rudolf et al. 2005). The datasets were analyzed for the boreal autumn (September, October, and November) mean, and anomalies in all variables were defined as deviations from the autumn climatological average (1961–1990).

Warm and cold episodes are based on a threshold of ± 0.5°C for Niño3.4 (5°S–5°N, 120°–170°W) SSTA in the autumn period. Although a zonal displacement of the action center occurs during El Niño, there is no significant change in its zonal location for La Niña events (Kug et al. 2009; Ren and Jin 2011). Therefore, all La Niña events may be classified into one category. Fourteen La Niña autumns were identified (1954, 1955, 1956, 1962, 1970, 1971, 1974, 1975, 1984, 1988, 1995, 1998, 1999, and 2007), which are largely consistent with the definition of the Climate Prediction Center. An analysis of the spatial distribution of combined SSTA and convection patterns identifies nine CT El Niño autumns (1951, 1957, 1963, 1965, 1972, 1976, 1982, 1987, and 1997) and nine WP El Niño autumns (1969, 1977, 1991, 1994, 2002, 2003, 2004, 2006, and 2009), which coincides with those of Zhang et al. (2011). Events having larger SSTA in the eastern Pacific, east of 150°W, are classified as CT El Niño autumns, whereas events with a larger SSTA located in the central Pacific or mid-western Pacific west of 150°W are grouped together as WP El Niño autumns. Some events (e.g., 1969 and 2006) show comparable intensities for SSTA in the central and far eastern Pacific, and these events are also defined as WP El Niño autumns, because the central Pacific warming is much more conducive to the formation of deep convection compared to the eastern Pacific warming resulting from a higher background SST. Among the nine WP El Niño autumns, five were defined in the study of Kim et al. (2009). Here, another four autumns (1977, 2003, 2006, and 2009) are also defined as WP El Niño autumns. The convective anomaly centers associated

with these four events are located over the western equatorial Pacific (not shown), which is similar to those of the WP El Niño, but different from those of the CT El Niño (Ashok et al. 2007; Weng et al. 2007; Kug et al. 2009). Therefore, considering the patterns of the SST and convection anomalies, it is reasonable to classify these four events into the WP El Niño autumns. However, five "dateline El Niño" autumns (1963, 1977, 1986, 1994, and 2003) are identified by Larkin and Harrison (2005a), which is very different from the definition in this study. This is because the spatial patterns are not considered in their study. Composite analysis is employed to investigate differences in climatic impact between the two types of El Niño, using Student's two-tailed significance test. The main conclusion is not sensitive to minor differences in the selection of the WP and CT El Niño events.

3. Teleconnections associated with the two types of El Nino

3.1 SSTA patterns and associated atmospheric responses in the tropical Pacific

For CT El Niño autumns, large positive SSTA covers the eastern to central tropical Pacific, and significant negative SSTA appears in the western tropical Pacific (Fig. 1a). However, for WP El Niño autumns, positive SSTA covers most of the tropics, with the maximum positive SSTA located in the central equatorial Pacific near the dateline (Fig. 1b). There is no significant negative SSTA in the equatorial western Pacific. Associated with the large differences in zonal location of the maximum SSTA over the tropical Pacific, different SSTA occurs in the Indian Ocean and extratropical Pacific. During the CT El Niño, weak warming and cooling SSTAs occur in the Indian Ocean, and in the North and South Pacific, respectively. During the WP El Niño, weak warming SSTA in the Indian Ocean and the North Pacific is noticed in the WP El Niño composite, as mentioned previously (e.g., Ashok et al. 2007; Kug et al. 2009). During La Niña autumns, the associated SSTA pattern is almost opposite to that of CT El Niño autumns (Fig. 1c), except that the SSTA intensity of the La Niña composite is weaker than that of the CT El Niño composite.

The tropical circulations associated with the two types of El Niño are expected to be distinct because of their differing SSTA patterns. Corresponding to the SSTA pattern of CT El Niño autumns, anomalous moisture convergence covers a broad area over the eastern to central equatorial Pacific, and anomalous moisture divergence occurs over the western equatorial Pacific (Fig. 2a). Rainfall may be enhanced in the eastern to central equatorial Pacific because of the large moisture convergence, which is similar to the results of previous studies (e.g., Wang et al. 2000). Along with the westward displacement of the maximum SSTA associated with the WP El Niño, the moisture convergence anomalies are also shifted westward and located in the area of 150°–175°E (Fig. 2b). There is almost no significant anomaly for the vertically integrated moisture divergence over the eastern to central equatorial Pacific. Therefore, the anomalously positive rainfall is also displaced westward, which is consistent with the study by Zhang et al. (2011).

As shown in Figure 1a and b, the intensity of the WP El Niño SSTA is weaker than that of the CT El Niño; however, the magnitude of their impact on the tropical Pacific climate is comparable in both cases. For example, although the spatial scale of moisture convergence is smaller during the WP El Niño than that during the CT El Niño, the amplitude in both cases is similar (Figs. 2a, b). This is because the SSTA in the central Pacific is much more effective in forming deep convection when compared with the eastern Pacific SSTA, given the higher background SST (Kim et al. 2009; Kug et al. 2009). In association with La Niña events, the tropical Pacific is dominated by anomalous moisture divergence (Fig. 2c), whereas significant moisture convergence anomalies appear over the far western and southwestern tropical Pacific.

3.2 Extratropical circulation anomalies over the North Pacific/North America region

In association with the two types of El Niño event, the contrast in their tropical circulation may result in large differences in the extratropical atmospheric circulation, since the tropical Pacific Ocean is a central driver of global circulation (Cane 1998). For the CT El Niño composite, the teleconnection patterns show a strengthening Aleutian Low (Fig. 3a), and the associated southwesterly anomalies in its southeastern area can bring moist air to the west coast of southern North America. In the northeastern part of the anomalous cyclone, the corresponding southeasterlies can inhibit the transport of moist air to the adjoining landmass. Most regions of North America are dominated by anomalously anticyclonic atmospheric circulations, but there is almost no SLP anomaly above a 0.1 confidence level. During autumn, the teleconnection pattern corresponding to the WP El Niño is different to that of the CT El Niño over the North Pacific (Fig. 3b), in that there are three anomalous centers in SLP and wind: anticyclone, cyclone, and anticyclone stretching from west to east, respectively. For one thing, the

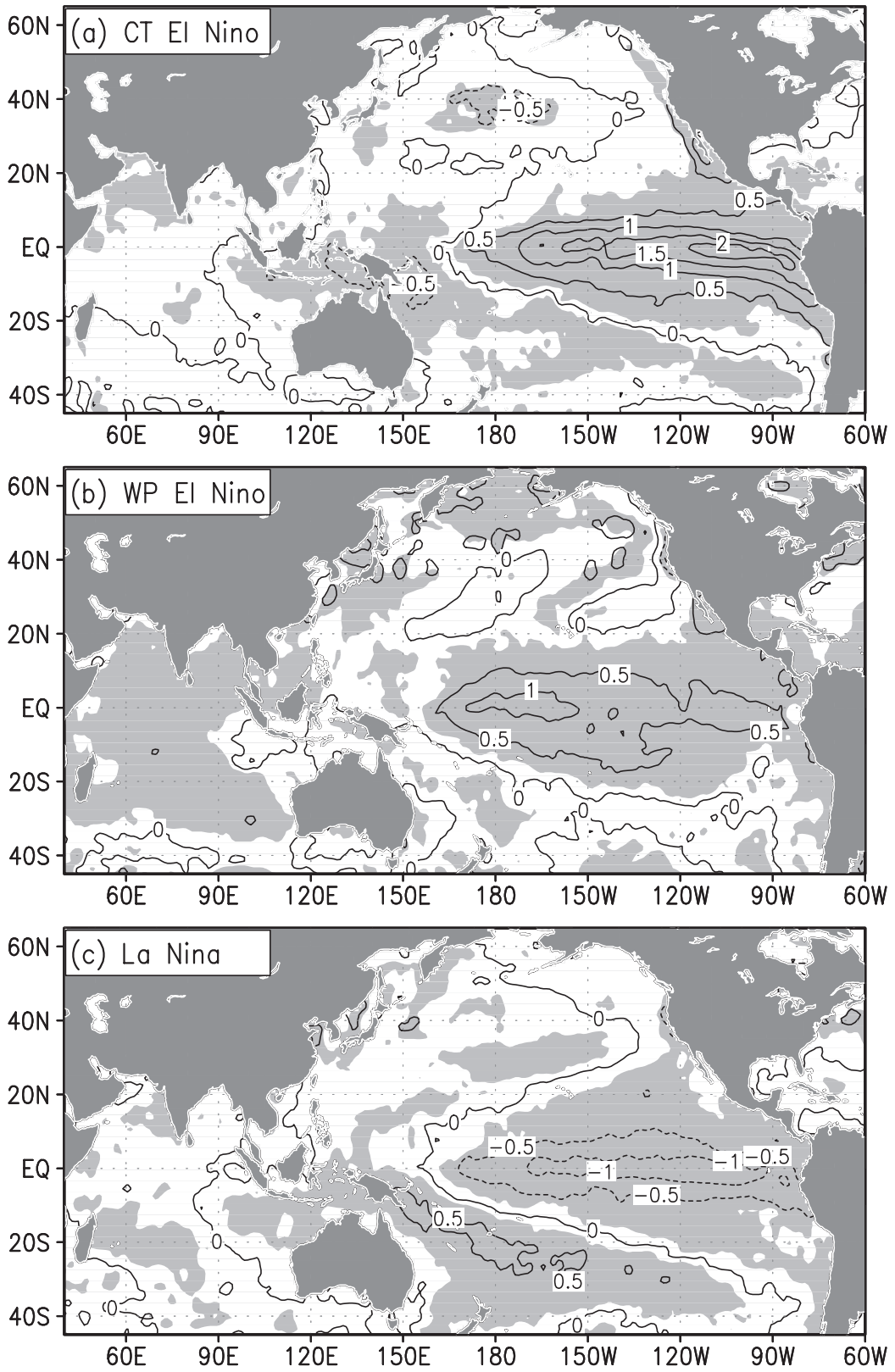

Fig. 1. Composite anomalies of SST (shading in °C) for CT El Niño (a), WP El Niño (b), and La Niña (c). Shading indicates that SST anomalies exceed the 0.05 confidence level.

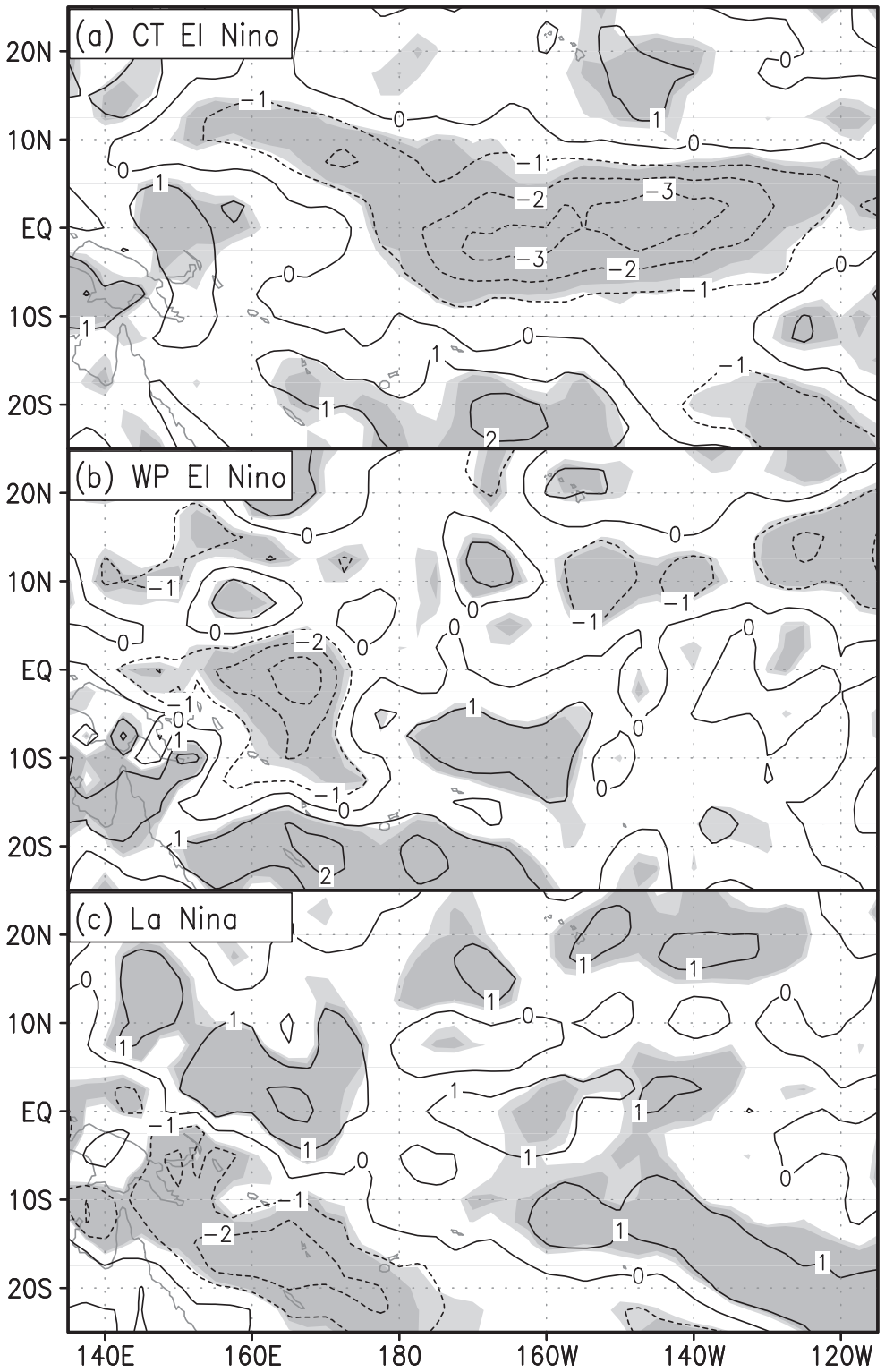

Fig. 2. Composite anomalies of vertically integrated moisture divergence (mm/d) based on CT El Niño (a), WP El Niño (b), and La Niña (c) events. Light (dark) shading indicates that the anomalies exceed the 0.1 (0.05) confidence level.

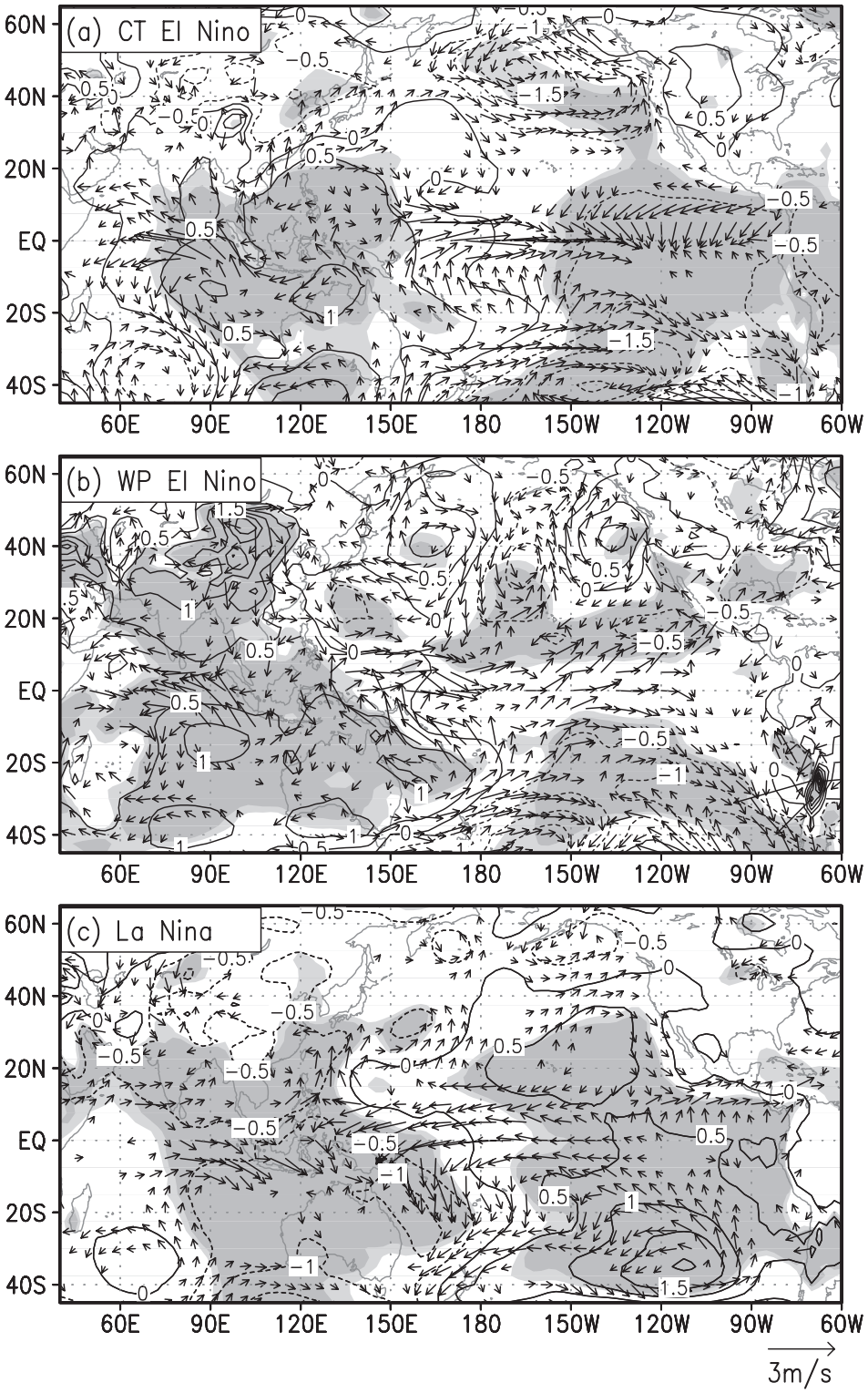

Fig. 3. Composite anomalies of SLP (contours in hPa) and surface wind (vectors in m/s) based on CT El Niño (a), WP El Niño (b), and La Niña (c) events. Light (dark) shading indicates that the SLP anomalies exceed the 0.1 (0.05) confidence level. Winds with speeds less than 0.3 m/s are not shown.

PNA pattern over the North Pacific is possibly shifted westward owing to the westward displacement of the warming SSTA center; additionally, the convection anomaly over the western Pacific associated with the WP El Niño can also influence the mid-latitude pattern through the Pacific-Japan teleconnection. Note that the SLP response over the North Pacific is weaker during the WP El Niño than during the CT El Niño. The anticyclonic anomaly near 40°N, 130°W can enhance the eastern Pacific Subtropical High, and the associated northwesterly wind anomalies, in the northern part of this anticyclone, tend to bring unusually moist air to northwestern North America. In the southeastern part of the anticyclone, anomalous northerlies and northeasterlies tend to cause an unusually dry climate over southwestern North America. Southeastern North America is dominated by a significant low-pressure anomaly, and the associated cyclonic circulation tends to bring moist air to the southeastern USA from the Gulf of Mexico and the Atlantic Ocean. In addition, the WNP circulation is very different during the two types of El Niño, as reported by Zhang et al. (2011). With regard to the La Niña phase, the associated atmospheric response is approximately opposite to that of the CT El Niño except for in the mid-latitude region near 50°N (Fig. 3c).

Furthermore, vertically integrated moisture flux and moisture divergence are shown in Fig. 4, to examine the moisture transport through the anomalous circulation for the two types of El Niño. Over the North Pacific, unusual cyclonic moisture transport is caused by the anomalous atmospheric circulation during the CT El Niño autumn (Fig. 4a). This anomalous moisture flux transports water vapor to the southwestern USA and reduces the eastward movement of water vapor from the North Pacific to the northwestern USA. Correspondingly, moisture convergence and divergence anomalies appear over the southwestern and northwestern USA, respectively. The mid-eastern USA is mainly covered by an anomalous northerly moisture flux, which tends to transport unusually dry air from the north, causing moisture divergence. The anomalous anticyclonic moisture transport associated with the WP El Niño generates wetter- and drier-than-normal climate over the coast of northwestern and southwestern North America, respectively (Fig. 4b), whereas the southeastern USA is dominated by anomalous cyclonic moisture transport and convergence. For the La Niña autumn, the anomalous moisture transport is almost opposite to that of the CT El Niño autumn (Fig. 4c); however, the La Niña and WP El Niño composites do show similar anomalies over some regions, such as the eastern North Pacific near 30°N.

3.3 Vertical structures

Figures 5 and 6 display the anomalous stream-function composites during the CT El Niño autumns at different vertical levels. The anomalies at the middle troposphere are not shown because they are similar to those at 300 hPa. We see that the anomalous cyclone over the North Pacific occurs at each level, with the strongest signal in the upper troposphere (Figs. 5–6a). This vertical structure is different to that over the WNP, which indicates that the anomalous WNP anticyclone in the lower troposphere (Fig. 5a) disappears in the middle and upper troposphere (Fig. 6a). Therefore, the PNA teleconnection patterns primarily display a barotropic structure, whereas the anomalous WNP circulation shows a baroclinic feature.

Consistent with Subsection 3.2, the stream-function composites show different responses to the WP and CT El Niño conditions over the North Pacific (Figs. 5a, b). The associated responses over the North Pacific in Fig. 3b are apparent in the stream-function composite at each vertical level during WP El Niño autumns (Figs. 5b, 6b). This anomaly pattern is stronger in the middle and upper troposphere than in the lower troposphere. Although the responses differ between the WP and CT El Niño in the boreal autumn, their vertical structures are consistent, in that the North Pacific has a barotropic feature and the WNP shows a baroclinic structure. As for La Niña autumns, their associated atmospheric anomalies are approximately opposite to those during the CT El Niño events at every level (Figs. 5c, 6c). These results are consistent with previous studies; for example, Ting (1996) pointed out that tropic heating can cause a baroclinic and barotropic response in the atmospheric circulation over the tropics and extratropics, respectively.

4. Regional autumn rainfall anomaly and decadal shift associated with ENSO

4.1 Autumn rainfall distribution and contribution

Figure 7 shows the annual rainfall distribution and the autumn percentage of the annual rainfall total over the USA. High annual rainfall occurs mainly in the eastern half of the contiguous USA and along west coast of the USA. In most areas, autumn rainfall is above 20% of the annual total except for a small area in the central, southwestern, and southeastern USA. Therefore, autumn rainfall is a considerable contributor to the annual rainfall, but more importantly, rainfall anomalies during autumn could cause significant economic losses because autumn is usually the harvest

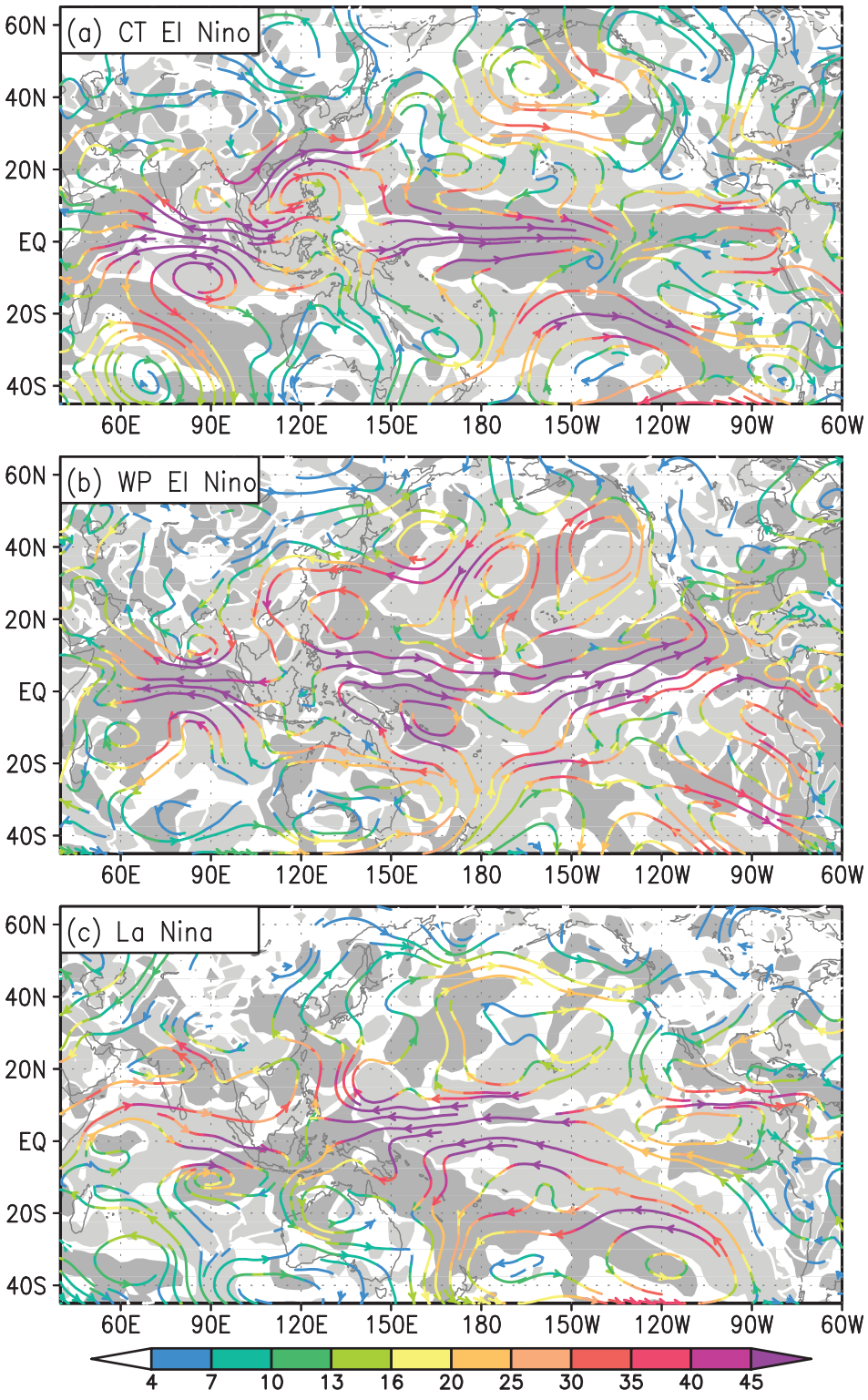

Fig. 4. Composite anomalies of vertically integrated moisture transport (streamlines in kg × m/s) and moisture divergence (shading in mm/d) based on CT El Niño (a), WP El Niño (b), and La Niña (c) events. Light (dark) shading indicates anomalies above (below) 0.2 (–0.2).

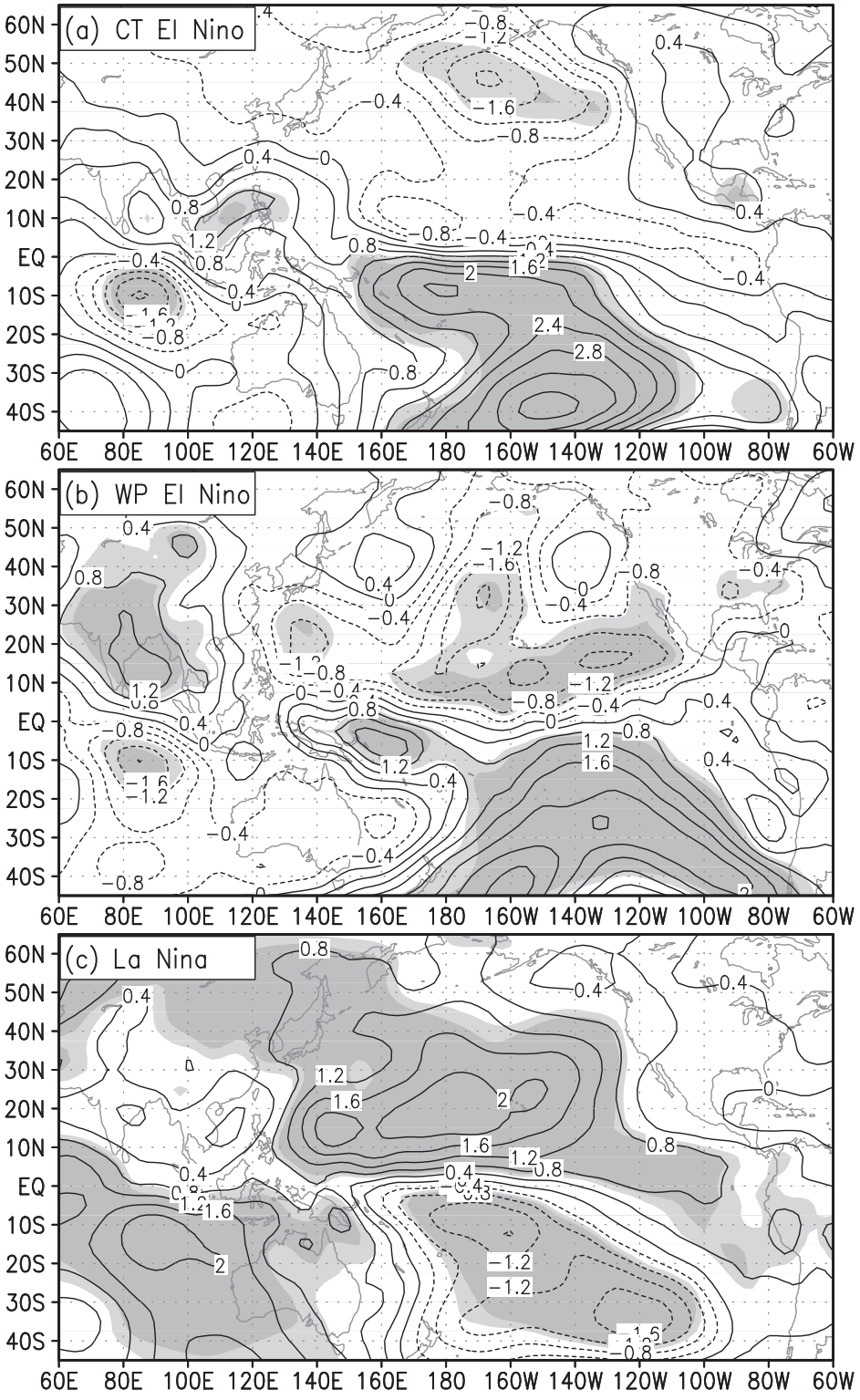

Fig. 5. Composite autumn mean stream-function (10^{-6} m^2/s) anomalies at 925 hPa for CT El Niño (a), WP El Niño (b), and La Niña (c). Light (dark) shading indicates that stream-function anomalies exceed the 0.1 (0.05) confidence level. The contour interval is 0.4.

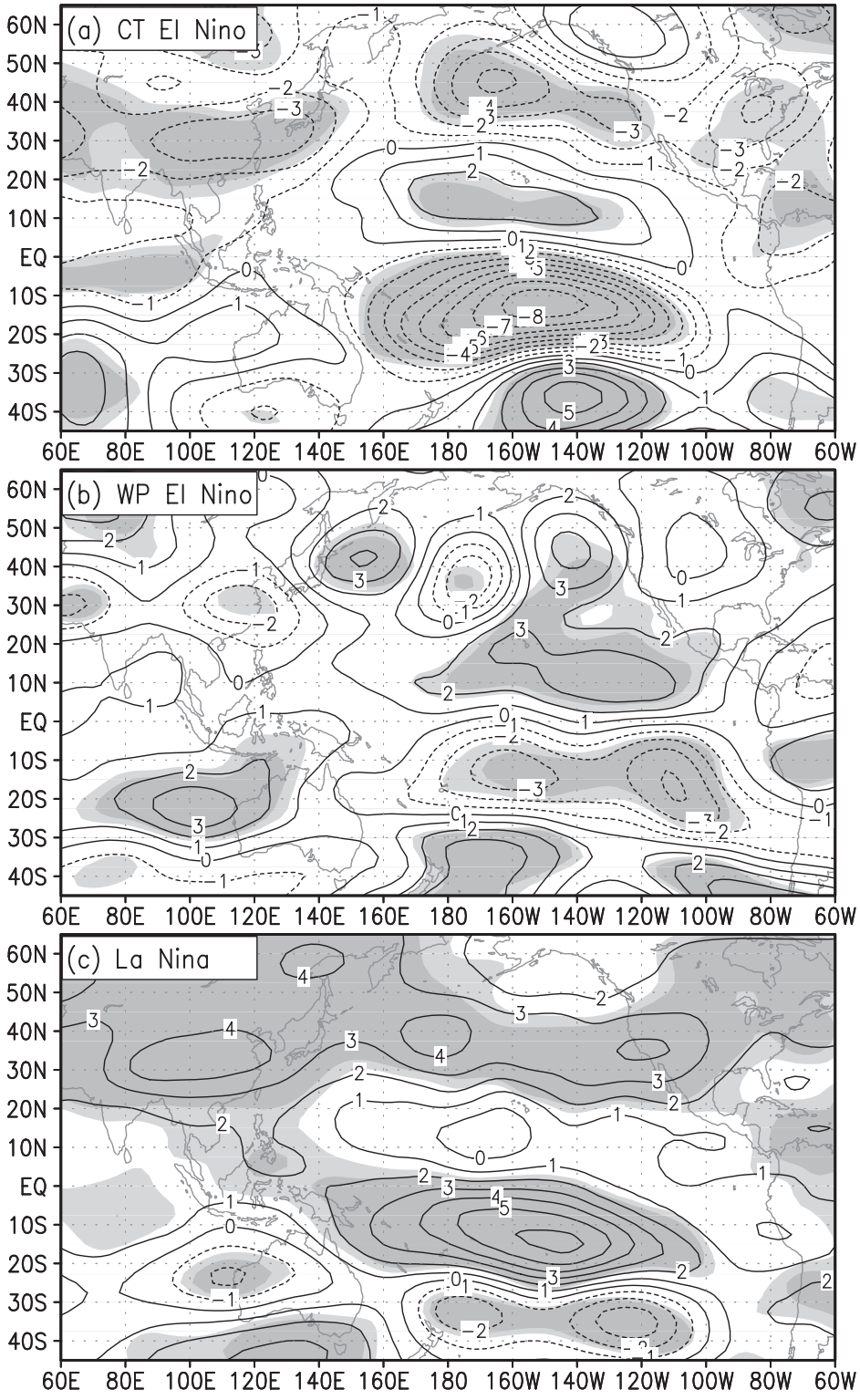

Fig. 6. As for Fig. 5, except for 300 hPa and a contour interval of 1.

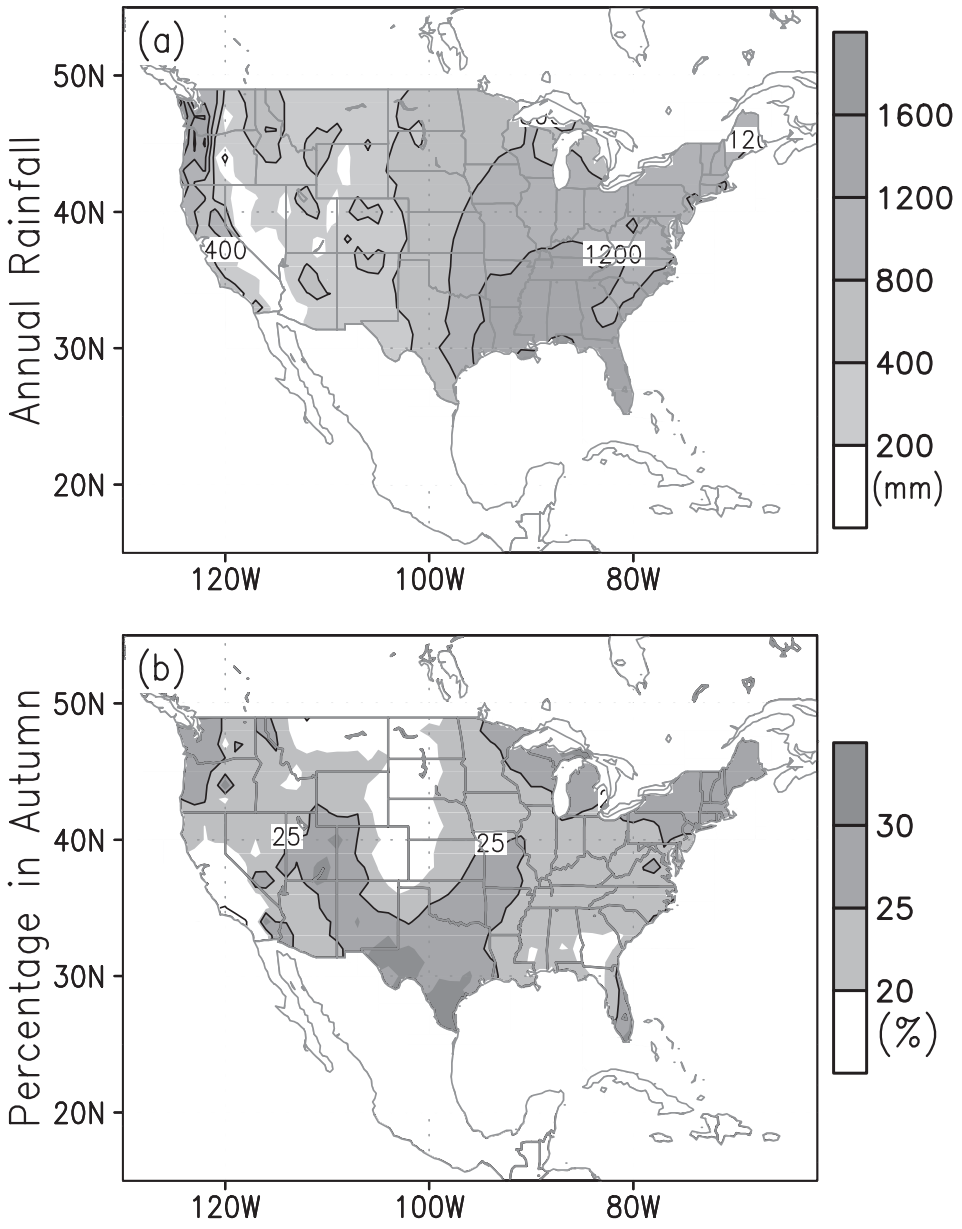

Fig. 7. Climatology of annual total rainfall (mm) (a) and percentage (%) of annual total rainfall in autumn (b). Contour interval in (a) is 400 mm.

season.

4.2 Rainfall anomalies during ENSO autumns

The different teleconnection patterns associated with the two types of El Niño (see Section 3) could be responsible for the different regional rainfall anomalies. In particular, the approximately opposing circulation anomaly patterns over the eastern North Pacific may result in diametric rainfall anomalies in adjoining countries. The rainfall anomalies in the USA show different patterns for the two types of El Niño (Fig. 8). During the CT El Niño, the rainfall anomalies show a surplus over the southwestern region and southeastern coast of the USA, and a deficit over the northwestern and mid-eastern USA (Fig. 8a). These rainfall anomalies in the USA are associated mainly with the PNA

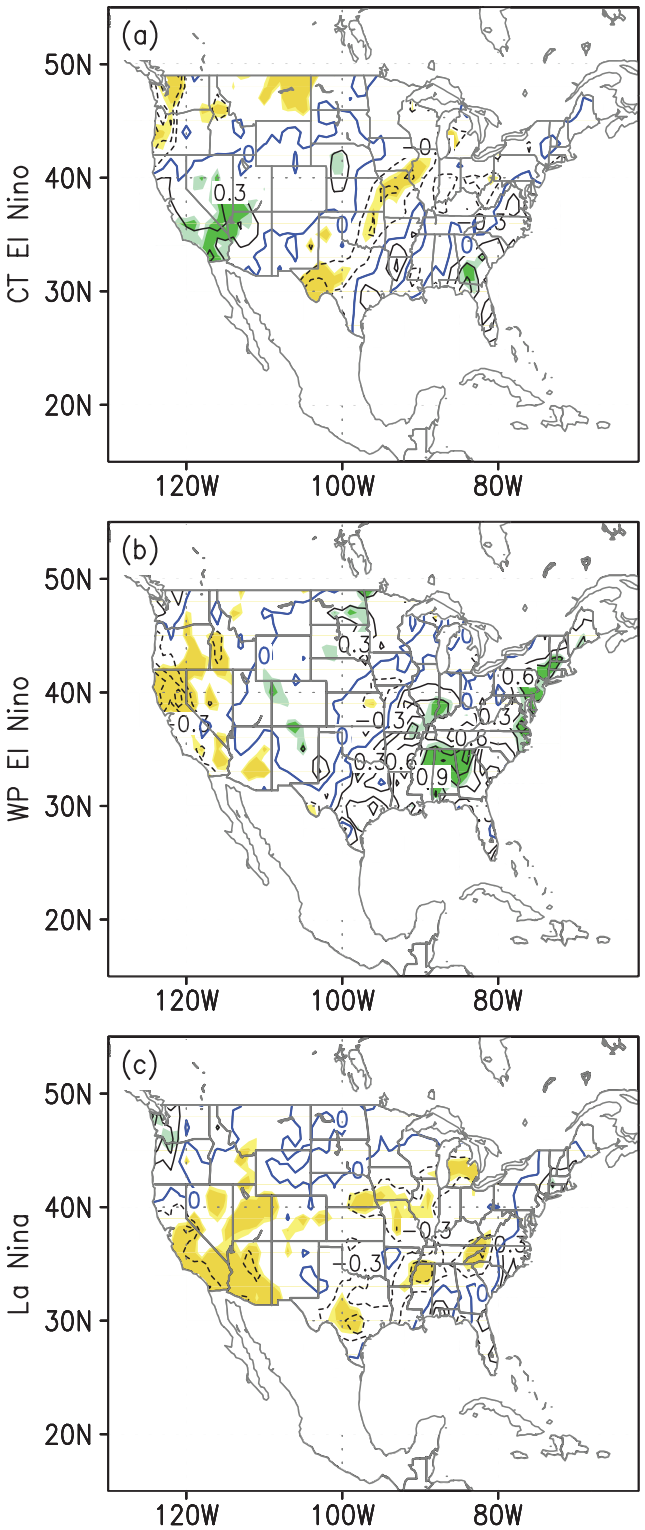

Fig. 8. Composites of rainfall (mm/d) anomalies for CT El Niño (a), WP El Niño (b), and La Niña (c) events. Light (dark) shading indicates that rainfall anomalies exceed the 0.1 (0.05) confidence level. Yellow (green) colors denote negative (positive) values. Contour interval is 0.3 and blue contours indicate a zero value.

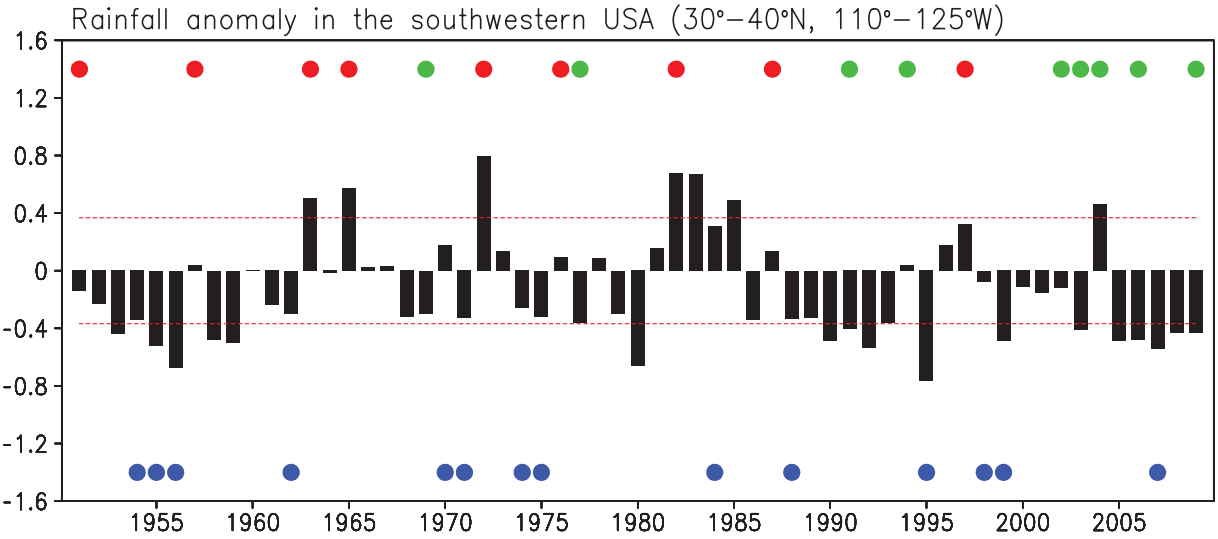

Fig. 9. Time series of regional rainfall anomalies (mm/d) in the southwestern USA (30°–40°N, 110°–125°W) during autumn. The red lines indicate one standard deviation of this averaged regional rainfall. Red, green, and blue dots indicate CT El Niño, WP El Niño, and La Niña events, respectively.

teleconnection patterns (Fig.s 3a, 4a). For example, the southwestern USA receives more autumn rainfall because the southwesterlies related to the anomalous cyclone over the North Pacific transport anomalously wet air to the southwestern USA. The autumn rainfall is reduced over the northwestern USA, since the anomalous southeasterlies inhibit the eastward transport of water vapor. For the WP El Niño, the western USA receives a rainfall deficit, whereas the mid-western and southeastern USA is dominated by a wetter autumn compared with the normal climate (Fig. 8b). Opposite rainfall responses to the two types of El Niño appear in the southwestern USA that coincide with the different teleconnection patterns over the eastern North Pacific (Figs. 3, 4). In addition, compared with the CT El Niño, the southeastern USA receives much more rainfall during the WP El Niño, which corresponds to anomalous cyclonic circulation (Fig. 3b) and moisture convergence (Fig. 4b).

During La Niña autumns, most areas of the USA receive rainfall deficits (Fig. 8c). Over the southwestern USA, the rainfall response to the La Niña condition is similar to that for the WP El Niño, and opposite to that for the CT El Niño. GPCC rainfall data show the same results for the autumn rainfall response to the different ENSO types (not shown).

4.3 Decadal changes in autumn rainfall

The zonal location of the air–sea action center has changed markedly for El Niño events since 1990; however, there has been no significant change in its zonal location associated with La Niña events (Kug et al. 2009; Ren et al. 2011). Therefore, the climate anomalies are highly variable during El Niño, whereas the climatic impact is relatively stable during La Niña for the past several decades. These ENSO changes may explain the regional rainfall differences, especially over sensitive regions such as the southwestern USA. To further investigate the decadal impact of ENSO on autumn rainfall, Fig. 9 shows a time-series of rainfall anomalies over the southwestern USA (30°–40°N, 110°–125°W) relative to the various ENSO events. The impact of La Niña on autumn rainfall has been relatively stable in the past six decades. Rainfall deficits appear in about 86% (12 of 14) of the La Niña autumns over the southwestern USA, including five severe rainfall deficits (anomalies exceeding one standard deviation). In contrast, during the warm phase of ENSO, the CT and WP types have strongly contrasting impacts on autumn rainfall over the southwestern USA. In eight of nine CT El Niño autumns, the region receives a rainfall surplus, with the anomalies exceeding one standard deviation for four events. However, the southwestern USA experiences rainfall deficits in seven of nine WP El Niño autumns, with four severe rainfall deficits.

Since the late twentieth century, the WP El Niño

has become more common, whereas the CT El Niño has become less frequent (Fig. 9). This change tends to result in more frequently recurrent autumn rainfall deficits in the southwestern USA. Thus, the regime change of El Niño may give rise to the decadal changes in regional autumn rainfall. As shown in Fig. 9, the autumn rainfall over the southwestern USA oscillates between surplus and deficit from the early 1960s to the late 1980s, whereas rainfall deficits have been dominant during the 1990s and 2000s. It is noticeable that autumn rainfall deficits were also dominant over the southwestern USA during the 1950s, possibly related to frequent occurrences of strong La Niña events. The reasons for these deficits deserve further exploration in the future, but in this study we have focused on the decadal change since the early 1990s, when WP El Niño events have occurred more frequently.

Figure 10a shows decadal differences in autumn rainfall over the USA between 1966–1985 and 1990–2009. The changes show a rough decrease in the west and mid-east, and an increase in the mid-west and southeast. To evaluate the contribution of ENSO to the decadal change, Figure 10b shows the autumn rainfall differences associated with ENSO events in these two periods. The ENSO-related rainfall differences are obtained from the average rainfall anomalies during all ENSO autumns in 1990–2009 minus those in 1966–1985. The rainfall difference patterns associated with ENSO are very similar to the total decadal difference. Therefore, the decadal changes in autumn rainfall over the southwestern USA are related to the ENSO decadal change. The decadal change in autumn rainfall is possibly affected by not only the El Nino changes but also the La Nina changes. We also found that La Nina further contributes, especially in the western USA (not shown). For example, although the autumn rainfall over the Southwestern USA shows deficits during the La Niña autumns in both two decades, their intensity seems to increase in the late period (Fig. 9).

5. Discussion and conclusion

We compared the teleconnection patterns associated with the CT and WP El Niño during the boreal autumn and their associated regional rainfall changes over the USA. The teleconnection patterns over the North Pacific differ corresponding to the two types of El Niño. During CT El Niño autumns, a strong anomalous cyclone emerges in the North Pacific. The anomalous southwesterlies associated with the North Pacific cyclonic anomalies tend to bring anomalously moist air to the west coast of the southwestern USA causing more rainfall. However, the anomalies over the North Pacific associated with the WP El Niño, produce anticyclonic, cyclonic, and anticyclonic anomalies from west to east. The anomalous anticyclone over the eastern North Pacific produces anomalous northerlies and northeasterlies over the southwestern USA, which tend to bring unusually dry air from high latitudes, reducing rainfall in the region. Therefore, the changes in teleconnection pattern produce opposing climatic impacts over the southwestern USA during the CT and WP El Niño autumns, as is also the case in southern China (Zhang et al. 2011). In addition, a significant difference in autumn rainfall appears over the southeastern USA, which receives more rainfall during the WP El Niño compared with the CT El Niño.

Larkin and Harrison (2005a) discussed differences in autumn rainfall associated with the two types of El Niño. Compared with their studies, most of the conventional El Niño events are consistently selected; however, there are large difference when selecting the WP El Niño events. For CT El Niño autumns, the rainfall anomalies found in this study are similar to those identified by Larkin and Harrison (2005a) over the western USA; whereas their study shows almost no significant anomalies in the eastern USA, which contrasts with the results of this paper. We found that the autumn rainfall response is more stable over the western USA than over the eastern USA. For the WP El Niño, a different pattern is displayed for the autumn rainfall anomalies in Larkin and Harrison (2005a), possibly due to the difference in events selected. In this study, event selection followed present mainstream approach based on the spatial patterns that are not considered in Larkin and Harrison (2005a)'s definition, giving different conclusions that are critical for the agricultural economy. Overall, the composites associated with the two types of El Niño show different rainfall anomalies in the USA. However, the rainfall composites are noisy and weak, possibly due to small numbers of samples and ENSO complexity. Some uncertainties exist regarding the impacts of ENSO on climate over the USA during autumn. For example, the southwestern USA experienced a rainfall surplus in 2004 (Fig. 9), which is not consistent with the typical WP El Niño. Consequently, factors other than ENSO need to be considered such as the North Pacific and Atlantic SST anomalies (e.g., McCabe et al. 2004; Sutton and Hodson 2005).

Autumn rainfall over the southwestern USA shows a decadal change, with a sharp decrease after 1990. This change is associated with more recurrent WP El Niño events and less frequent CT El Niño events. Moreover, the WP El Niño may become more common under the influence of global warming (Yeh et al. 2009), which

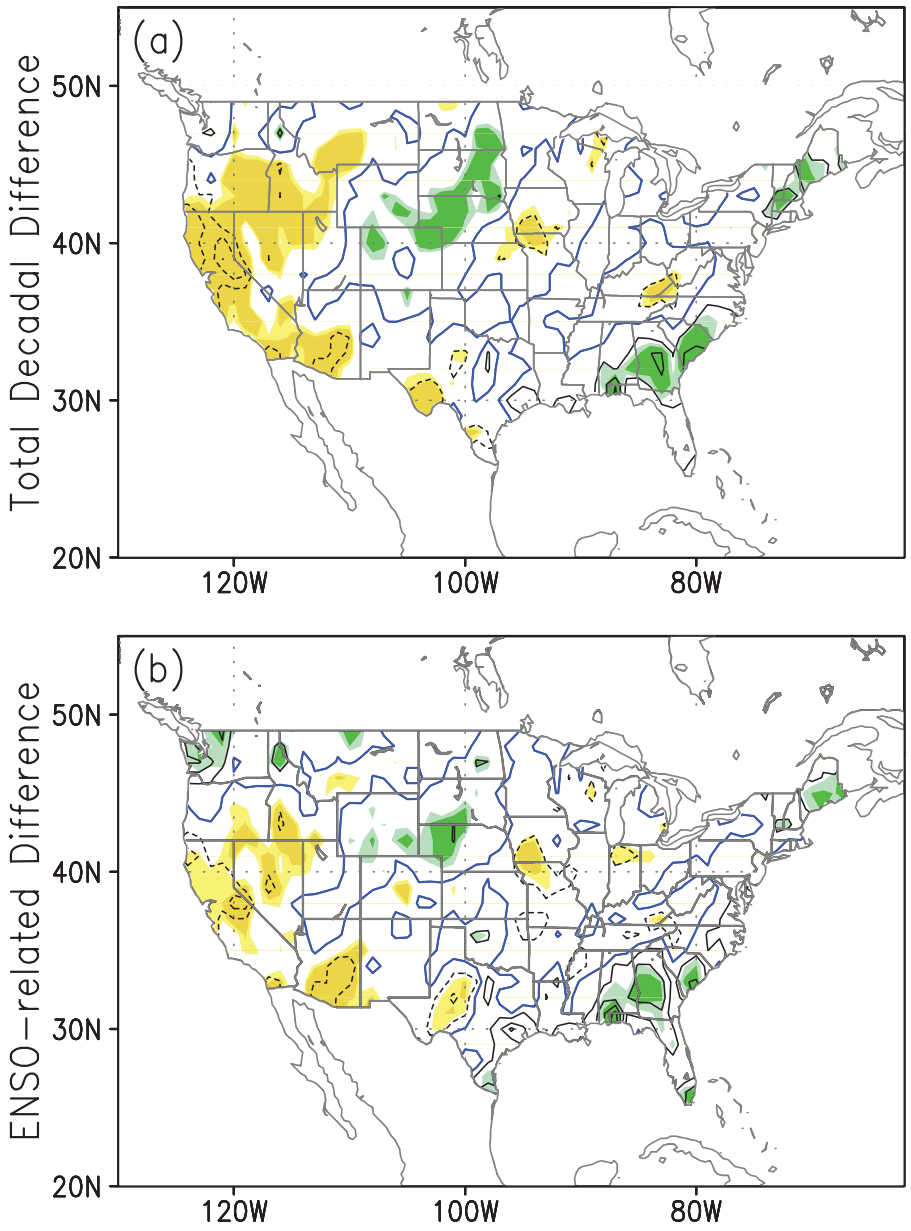

Fig. 10. (a) Total decadal difference of autumn rainfall (mm/d) between 1966–1985 and 1990–2009. (b) Decadal difference of autumn rainfall (mm/d) associated with ENSO events between 1966–1985 and 1990–2009. The contour interval is 0.4 mm/d and blue contours indicate a zero value. Yellow (green) colors denote negative (positive) values, and light (dark) shading indicates that the anomalies exceed the 0.1 (0.05) confidence level.

could lead to increasingly frequent shortages of autumn rainfall over the southwestern USA.

Acknowledgements

We appreciate the helpful comments and suggestions from the anonymous reviewers. This work is jointly supported by the National Basic Research Program "973" (Grant No. 2010CB950400), the National Nature Science Foundation of China (41005049, 40805028), National Science Foundation grants ATM 1034798, NOAA grand NA10OAR4310200, and DOE grant DESC0005110.

References

Ashok, K., S. K. Behera, S. A. Rao, H. Weng, and T. Yamagata, 2007: El Niño Modoki and its possible teleconnection. *J. Geophys. Res.*, **112**, C11007, doi:10.1029/2006JC003798.

Battisti, D. S., and A. C. Hirst, 1989: Interannual variability in a tropical atmosphere-ocean system: influence of the basic state, ocean geometry, and non-linearity. *J. Atmos. Sci.*, **46**, 1687–1712.

Bejarano, L., and F.-F. Jin, 2008: Coexistence of equatorial coupled modes of ENSO. *J. Climate*, **21**, 3051–3067.

Bjerknes, J., 1969: Atmospheric teleconnections from the equatorial Pacific. *Mon. Wea. Rev.*, **97**, 163–172.

Cai, W., and T. Cowan, 2009: La Niña Modoki impacts Australia autumn rainfall variability. *Geophys. Res. Lett.*, **36**, L12805, doi:10.1029/2009GL037885.

Cane, M. A., 1998: Climate change: A role for the tropical Pacific. *Science*, **282**, 59–61.

Cane, M. A., and S. E. Zebiak, 1985: A theory for El Niño and the Southern Oscillation. *Science*, **228**, 1085–1087.

Chen, G., and C.-Y. Tam, 2010: Different impacts of two kinds of Pacific Ocean warming on tropical cyclone frequency over the western North Pacific. *Geophys. Res. Lett.*, **37**, L01803, doi:10.1029/2009GL041708.

Feng, J., L. Wang, W. Chen, S. K. Fong, and K. C. Leong, 2010: Different impacts of two types of Pacific Ocean warming on Southeast Asia rainfall during boreal winter. *J. Geophys. Res.*, **115**, D24122, doi:10.1029/2010JD014761.

Feng J., and J. Li, 2011: Influence of El Niño Modoki on spring rainfall over South China. *J. Geophys., Res.*, **116**, doi:10.1029/2010JD015160.

Hong, C.-C., Li, Y.-H., Li, T., and Lee M.-Y., 2011: Impacts of central Pacific and eastern Pacific El Niño on tropical cyclone tracks over the western North Pacific, *Geophys., Res. Lett.,* **38**, doi:10/1029/2011GL048821.

Hoskins, B. J., and D. J. Karoly, 1981: The steady linear response of a spherical atmosphere to thermal and orographic forcing. *J. Atmos. Sci.*, **38**, 1179–1196.

Jin, F.-F., 1997a: An equatorial ocean recharge paradigm for ENSO. Part I: Conceptual model. *J. Atmos. Sci.*, **54**, 811–829.

Jin, F.-F., 1997b: An equatorial ocean recharge paradigm for ENSO. Part II: A stripped-down coupled model. *J. Atmos. Sci.*, **54**, 830–847.

Jin, F.-F., J.-S. Kug, S.-I. An, and I.-S. Kang, 2003: A near-annual coupled ocean-atmosphere mode in the equatorial Pacific Ocean. *Geophys. Res. Lett.*, **30**, 1080, doi:10.1029/2002GL015983.

Kalnay, E., and Coauthors, 1996: The NCEP/NCAR 40-year reanalysis project. *Bull. Amer. Meteor. Soc.*, **77**, 437–471.

Kao, H.-Y., and J.-Y. Yu, 2009: Contrasting eastern-Pacific and central-Pacific types of ENSO. *J. Climate*, **22**, 615–632.

Karl, T. R., C. N. Williams, Jr., F. T. Quinlan, and T. A. Boden, 1990: United States Historical Climatology Network (HCN) Serial Temperature and Precipitation Data, Environmental Science Division, Publication No. 3404, Carbon Dioxide Information and Analysis Center, Oak Ridge National Laboratory, Oak Ridge, TN, 389 pp.

Kim, H.-M., P. J. Webster, and J. A. Curry, 2009: Impact of shifting patterns of Pacific Ocean warming on North Atlantic tropical cyclones. *Science*, **325**, 77–80.

Kug, J.-S., F.-F. Jin, and S.-I., An, 2009: Two types of El Niño events: Cold tongue El Niño and warm pool El Niño. *J. Climate*, **22**, 1499–1515.

Larkin, N. K., and D. E. Harrison, 2001: Tropical Pacific ENSO cold events, 1946–95: SST, SLP, and surface wind composite anomalies. *J. Climate*, **14**, 3904–3931.

Larkin, N. K., and D. E. Harrison, 2005a: On the definition of El Niño and associated seasonal average U.S. weather anomalies. *Geophys. Res. Lett.*, **32**, L13705, doi:10.1029/2005GL022738.

Larkin, N. K., and D. E. Harrison, 2005b: Global seasonal temperature and precipitation anomalies during El Niño autumn and winter. *Geophys. Res. Lett.*, **32**, L16705, doi:10.1029/2005GL022860.

McCabe, G. J., M. A. Palecki, and J. L. Betancourt, 2004: Pacific and Atlantic Ocean influences on multidecadal drought frequency in the United States. *Proc. Natl. Acad. Sci.*, **101**, 4136–4141.

Mo, K. C., 2010: Interdecadal modulation of the impact of ENSO on precipitation and temperature over the United States. *J. Climate*, **23**, 3639–3656.

Neelin, J. D., D. S. Battisti, A. C. Hirst, F.-F. Jin, Y. Wakata, T. Yamagata, and S. E. Zebiak, 1998: ENSO theory. *J. Geophys. Res.*, **103**, 14,261–14,290.

Niu, N., and J. Li, 2008: Interannual variability of autumn precipitation over South China and its relation to atmospheric circulation and SST anomalies. *Adv. Atmos. Sci.*, **25**, 117–125.

Rayner, N. A., D. E. Parker, E. B. Horton, C. K. Folland, L. V. Alexander, D. P. Rowell, E. C. Kent, and A. Kaplan, 2003: Global analyses of sea surface temperature, sea ice, and night marine air temperature since the late nineteenth century. *J. Geophys. Res.*, **108**, No. D14, 4407, doi:10.1029/2002JD002670.

Rasmusson, E. M., and T. H. Carpenter, 1982: Variations in tropical sea surface temperature and surface wind fields associated with the Southern Oscillation/El Niño. *Mon. Wea. Rev.*, **110**, 354–384.

Ren, H.-L., and F.-F. Jin, 2011: Niño indices for two types of ENSO. *Geophys. Res. Lett.,* **38**, L04704, doi:10.1029/2010GL046031.

Ropelewski, C. F., and M. S. Halpert, 1987: Global and regional scale precipitation patterns associated with the El Niño/Southern Oscillation. *Mon. Wea. Rev.*, **115**, 1606–1626.

Ropelewski, C. F., and M. S. Halpert, 1996: Quantifying Southern Oscillation-precipitation relationships. *J. Climate*, **9**, 1043–1059.

Rudolf, B., C. Beck, J. Grieser, and U. Schneider, 2005: Global precipitation analysis products. Global Precipitation Climatology Centre (GPCC), DWD, Internet publication, 1–8.

Schopf, P. S., and M. J. Suarez, 1988: Vacillations in a coupled ocean-atmosphere model. *J. Atmos. Sci.*, **45**, 549–566.

Sutton, R. T., and D. L. R. Hodson, 2005: Atlantic Ocean forcing of North American and European summer climate. *Science*, **309**, 115–118.

Taschetto, A. S., and M. H. England, 2009: El Niño Modoki impacts on Australian rainfall. *J. Climate*, **22**, 3167–3174.

Ting, M., 1996: Steady linear response to tropical heating in barotropic and baroclinic models. *J. Atmos. Sci.*, **53**, 1698–1709.

Trenberth, K. E., and J. M. Caron, 2000: The Southern Oscillation revisited: Sea level pressure, surface temperatures, and precipitation. *J. Climate*, **13**, 4358–4365.

Trenberth, K. E., and D. P. Stepaniak, 2001: Indices of El Niño evolution. *J. Climate*, **14**, 1697–1701.

Van Loon, H., and R. A. Madden, 1981: The Southern Oscillation. Part I: Global associations with pressure and temperature in northern winter. *Mon. Wea. Rev.*, **109**, 1150–1162.

Wallace, J. M., and D. S. Gutzler, 1981: Teleconnections in the geopotential field during the Northern Hemisphere winter . *Mon. Wea. Rev.*, **109**, 784–812.

Wallace, J. M., E. M. Rasmusson, T. P. Mitchell, V. E. Kousky, E. S. Sarachik, and H. Von Storch, 1998: On the structure and evolution of ENSO-related climate variability in the tropical Pacific: Lessons from TOGA. *J. Geophys. Res.*, **103**, 14,169–14,240.

Wang, B., R. Wu, and X. Fu, 2000: Pacific-East Asian teleconnection: How does ENSO affect East Asian climate? *J. Climate*, **13**, 1517–1536.

Wang, C., and J. Picaut, 2004: Understanding ENSO physics – A review. In Earth's Climate: The Ocean-Atmosphere Interaction. C. Wang, S.-P. Xie, and J. A. Carton, Eds., *AGU Geophysical Monograph Series*, **147**, 21–28.

Wang, G., and H. H. Hendon, 2007: Sensitivity of Australia rainfall to inter-El Niño variations. *J. Climate*, **20**, 4211–4226.

Weng, H., K. Ashok, S. K. Behera, S. A. Rao, and T. Yamagata, 2007: Impacts of recent El Niño Modoki on dry/wet conditions in the Pacific rim during boreal summer. *Climate Dyn.*, **29**, 113–129.

Weng, H., S. K. Behera, and T. Yamagata, 2009: Anomalous winter climate conditions in the Pacific rim during recent El Niño Modoki and El Niño events. *Climate Dyn.*, **32**, 663–674.

Wyrtki, K., 1975: El Niño–The dynamic response of the equatorial Pacific Ocean to atmosphere forcing. *J. Phys. Oceanogr.*, **5**, 572–584.

Yeh, S.-W., J.-S. Kug, B. Dewitte, M.-H. Kwon, B. P. Kirtman, and F.-F. Jin, 2009: El Niño in a changing climate. *Nature*, **461**, 511–514.

Zhang, W., F.-F. Jin, J. Li, and H.-L. Ren, 2011: Contrasting impacts of two-type El Niño over the western North Pacific. *J. Meteor. Soc. Japan*, **89**, 563–569.

Zhang, W., J. Li, and F.-F. Jin, 2009: Spatial and temporal features of ENSO meridional scales. *Geophys. Res. Lett.*, **36**, L15605, doi: 1029/2009GL038672.